

# **Particulate matter pollution from a small coke-burning factory: soil magnetic screening and its relation with a simple atmospheric dispersion model**

JOSÉ D. GARGIULO AND MARCOS A.E. CHAPARRO

Centro de Investigaciones en Física e Ingeniería del Centro de la Provincia de Buenos Aires (CIFICEN, CONICET-UNCPBA), Pinto 399, 7000 Tandil, Argentina (jdgargiulo@gmail.com)

*Received: June 24, 2015; Revised: November 5, 2015; Accepted: December 6, 2015*

---

## **ABSTRACT**

*Coal combustion processes lead to release of gases and particulate matter (PM) into the atmosphere that are often harmful to human health. These airborne pollutants seem to be dispersed and deposited in soils mainly according to the prevailing atmospheric conditions. Several trace elements can be found attached to PM as well as Fe-rich magnetic particles that can produce magnetic enhancement in the uppermost soil horizons. In the present work, we use a simple Gaussian Dispersion Model (GDM) for modelling the distribution of fine PM emission coming from a small coal (coke) burning factory in order to evaluate the relationship between such modelled data (PM distribution) and measured data (soil magnetic properties and trace metal contents). Our results show a strong spatial variation of concentration-dependent magnetic parameters based on a uniform magnetomineralogy in the overall study area. In addition, these results were analysed using multivariate statistics for 13 magnetic and chemical variables and the GDM results for two different atmospheric stability classes, and hence the in-situ magnetic susceptibility, anhysteretic and saturation remanent magnetization showed positive and statistically significant correlation with the GDM results ( $R = 0.70$ ). Therefore, these results demonstrate the usefulness of magnetic properties in monitoring the PM distribution in soils or other environmental PM collectors.*

**Keywords:** magnetic parameters, heavy metals, Gaussian dispersion model, multivariate statistics, coke burning plant

## **1. INTRODUCTION**

Air pollution is perhaps one of the most important environmental problems within industrialized and urbanized areas. Toxic gases, small size particulate matter and fly ash are released into the atmosphere by industries, vehicles and home heating, among other pollution sources. These pollutants may include toxic elements such as heavy metals and polycyclic aromatic hydrocarbons (PAHs) (Conner *et al.*, 2001; Liu *et al.*, 2013). Such airborne pollutants are transported, diffused and accumulated far away from their sources

according to the local atmospheric conditions, i.e. mainly meteorological and circulation patterns. Therefore, the study of spatial and temporal distribution of airborne particulates generated by industrial processes is crucial to keeping human health safe in the long term. Petroleum coke (both green and calcined) is a black solid produced by the high pressure thermal decomposition of heavy (high boiling) petroleum process streams and residues. Green coke is the initial product formed during the cracking and carbonization of feedstocks used to produce a substance with a high carbon-to-hydrogen ratio. Green coke may undergo additional thermal processing at very high temperatures to produce calcined coke. The additional processing required to form calcined coke removes most of the remaining volatile matter (< 0.5%), thereby increasing the percentage of elemental carbon and the relative abundance of metals. The latter heating stage is applied in the Tandil Coke Factory analysed here. The particulate matter emission from these factories comprises particles with a variety of grain size, morphology and composition, which may be inhaled by humans and/or deposited in soils and vegetation located near the pollution source. In this type of industry, several gases, vapours and chemical trace elements are produced, including dangerous compounds for human health, such as, benzene, toluene and xylene (BTX). On the other hand, in detached PM a wide range of trace elements is found such as As, B, Br, Cr, Cu, Fe, Hg, Mo, Ni, Pb, Ti, V, Zn among others (*Hower et al., 2005*). Some of these heavy metals are characteristics of the coking process, such as Ni and V and they are present in fly ash (*Henke, 2005; Nelson, 1970*).

Magnetic mineralogy studies have been successfully developed in recent years, starting with studies from the 1980s (*Hunt et al., 1984; Thompson and Oldfield, 1986*). Ferrimagnetic iron oxide particles (mainly magnetite and maghemite) in fly ash, originating during high-temperature combustion of fossil fuels, are potentially the most significant source of magnetic enhancement found in the upper soil horizons (*Flanders, 1994; Strzyszcz et al., 1996; Ćurża, 1999; Magiera et al., 2006*). Several authors have examined the effectiveness of this method to study pollution in different environments, obtaining positive results (*Kapička et al., 1999; Schibler et al., 2002; Jordanova et al., 2003; Chaparro et al., 2006, 2007, 2012; Maher et al., 2008; Blundell et al., 2009; Bidegain et al., 2011; Rachwał et al., 2015*).

Magnetic measurement devices are able to detect very low ferromagnetic mineral concentrations in soils and sediments, which is an important advantage in detecting industrial pollution. In addition, several studies have found a similar distribution of magnetic particles and heavy metals around industrial sites, and hence significant correlations between magnetic and chemical variables. A number of authors have studied the association of magnetic parameters and anthropogenic heavy metals content in soils, for example, in Poland (*Strzyszcz, 1993; Strzyszcz et al., 1996; Heller et al., 1998*), in Austria (*Hanesch et al., 2002*), in the UK (*Charlesworth and Lees, 2001*), in Argentina and Antarctica (*Chaparro, 2006; Chaparro et al., 2007*), and in China (*Lu and Bai, 2006*).

During this study, we analyse the fine PM emission and deposition from a small coke factory using magnetic measurements in the soil. Magnetic parameters were statistically correlated with chemical measurements and with results of the plume dispersion model. For the latter, the modelled results were chosen according to the same geographic position as the sampling. Geostatistic methods (Moran's index and associated correlograms) were calculated for a spatial dependence analysis. Thus, the aim of this study was to: a) determine the soil's magnetic properties; b) evaluate the use of magnetic properties for

monitoring the PM distribution; and c) evaluate the effectiveness of magnetic methods contrasting with trace metal measurements and the modelled spatial PM distribution obtained with a Plume GDM type.

## 2. THE STUDY AREA AND SAMPLE COLLECTION

Tandil ( $37^{\circ}17'22''S$ ;  $59^{\circ}11'47''W$ , Argentina) is located in the southeastern part of Buenos Aires province, Argentina (Fig. 1). The weather is slightly damp; the annual mean temperature is  $13.4^{\circ}C$ , and the highest temperature is reached in January (mean  $20.6^{\circ}C$ ) and the lowest one in July (mean  $6.8^{\circ}C$ ). The wind does not have a strong preferential direction in annual periods. The mean speed is  $3.78$  m/s, higher from the South ( $4.81$  m/s) than from the North ( $3.36$  m/s). The speed distribution shows that the wind speed is in the range of  $2\text{--}5$  m/s for  $66.6\%$  of the days, above  $6$  m/s for  $24.3\%$  of the days, and below  $2$  m/s for  $9.1\%$  of the days. According to the Pasquill-Gifford classification (*Pasquill, 1961; Gifford, 1961*), the predominant atmospheric stabilities for Tandil are identified as type C and D, that is, between slightly stable and slightly unstable conditions.

The study area ( $\sim 5$  km $^2$ ) comprises soils for which the main land use is rural and the topographic pattern is quite regular; there are no important elevations or depressions. This fact is very important to satisfy the GDM's assumption with respect to the terrain complexity.

Soils in this area have developed from loess material, which covered the Tandilia system and has about one metre of depth. These soils have been classified as Luvic Phaeozem according to the WRB soil classification (also classified as Argiudolls according to the Soil's Taxonomy classification from the US Department of Agriculture (*Pazos, 1996; Pazos and Mastelan, 2001*), and they present a humus-rich superficial

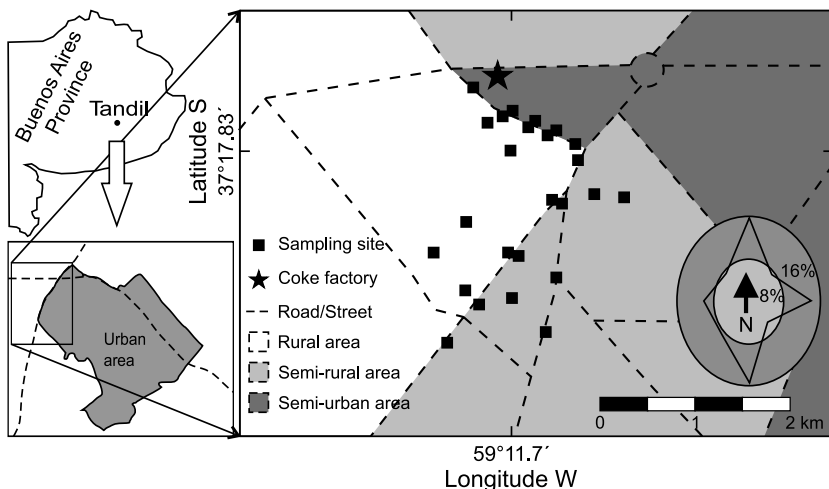


**Fig. 1.** Map of the study area (Tandil, Argentina) and distribution of sampling sites. The wind rose is for the 1991–2011 period.

horizon (0–10 cm) developed over mollic horizon of variable depth (10–50 cm). Then, they exhibit a layer of clay accumulation (hiper-petrocalcic horizon) from a depth of about 50–70 cm.

Topsoil sampling and in-situ magnetic susceptibility ( $\kappa_{\text{IS}}$ ) measurements were done for  $N = 27$  sites (Fig. 1). Samples were taken far enough away from roads (at least 10 m), over anthropogenic undisturbed areas. In-situ magnetic susceptibility readings at each site were done ( $n = 15$ ) and then averaged. Bulk topsoil samples of about 0.5 kg were collected at each site for measurements in the laboratory. At each sampling point, the top-soil layer (2 cm, horizon A) was collected by a stainless steel trowel and stored in a plastic bag. In the laboratory, each sample was dried at room temperature and sieved through a 2-mm steel mesh. A dust sample from the coke factory was also obtained for comparison purposes with the soils samples; this sample was collected from a soil close to the factory.

### 3. METHODS

#### 3.1. Atmospheric dispersion analysis

The PM dispersion was studied using a simple air pollution model GDM. This model provides the ground-level PM concentrations for point sources and is calculated using Eq. (1). At each geographic sampling point, the relative concentration was calculated taking into account six possible wind directions (W, WNW, NW, N, ENE and NE) and meteorological statistical data from Tandil city over a 20-year period, i.e. 1991–2011.

The GDM at ground-level can be written as follows:

$$C(x, y, z) = \frac{Q}{2\pi u \sigma_y \sigma_z} \exp\left(-\frac{y^2}{2\sigma_y^2} - \frac{H^2}{2\sigma_z^2}\right), \quad (1)$$

where  $C(x, y, z)$  is the concentration at a particular location,  $Q$  is the emission rate or the source strength,  $u$  is the mean wind speed in the considered period and  $H$  is the effective height of the PM release. Here,  $x$  is the distance along the wind direction,  $y$  is the distance along the horizontal crosswind direction, and  $z$  is the distance along the vertical axis.  $\sigma_y$  and  $\sigma_z$  are the standard deviation in the horizontal crosswind and vertical directions, respectively. These two parameters were defined empirically using the pair of formulas as follows (Martin, 1976):

$$\sigma_y = ax^b, \quad \sigma_z = cx^d + f, \quad (2)$$

where  $a, b, c, d$  and  $f$  are defined according to the stability type.

This model assumes no chemical reaction, continuous emission during the time of modelling and surface reflection. Furthermore, for the PM emission, it was considered that particles  $< 10 \mu\text{m}$  in size behave as gases; such assumption is based on a negligible PM sedimentation rate with respect to the wind velocity for small modelled distances in the wind direction.

In this GDM, only the  $Q$  parameter was unknown; however, this value does not affect the pattern of the spatial distribution and hence normalized values could be used.

### 3.2. Magnetic measurements

Different magnetic parameters were measured in the Paleomagnetic and Environmental Magnetism laboratory in Tandil (CIFICEN, Argentina). Measurements of volume-specific magnetic susceptibility in the laboratory ( $\kappa$ ) and in the field ( $\kappa_{ls}$ ), anhysteretic remanent magnetization ( $ARM$ ) and isothermal remanent magnetization ( $IRM$ ) were carried out. These are magnetic concentration-dependent parameters and consequently their values depend on the content of magnetic fraction in the sample.

The  $\kappa$  was measured at low frequency (470 Hz;  $\kappa_{lf}$ ) and high frequency (4700 Hz;  $\kappa_{hf}$ ), respectively, and the mass-specific susceptibility ( $\chi$ ) was calculated as  $\kappa/\rho$ , where  $\rho$  means density (assuming standard measurement volume of 10 cm<sup>3</sup> and mass of the specimen). Frequency-dependent susceptibility ( $\kappa_{fd\%}$ ), which indicates the presence of superparamagnetic (SP) grains, was calculated as  $\kappa_{fd\%} = (\kappa_{lf} - \kappa_{hf})/\kappa_{lf}$ , expressed in %. The  $ARM$  was measured after the sample was magnetized using a partial  $ARM$  (p $ARM$ ) device attached to a shielded demagnetizer (Molspin Ltd.). The peak AF used was 100 mT and the DC bias was 90  $\mu$ T. The anhysteretic susceptibility ( $\kappa_{ARM}$ ) was determined using DC field between of 10, 50 and 90  $\mu$ T and calculated by slope of linear regression through the obtained points. The  $IRM$  was measured after a series of forward fields (4–2500 mT using a pulse magnetizer model IM-10-30, ASC Scientific). Saturation isothermal remanent magnetization ( $SIRM$ ) was produced at a field of ~2500 mT. All remanence-carrying magnetic grains will make a contribution to the  $SIRM$ . Backfield magnetization in steps until a field of -300 mT was applied to the samples, allowing us to calculate the remanent coercivity ( $H_{cr}$ ) and the  $S$ -ratio defined as  $-IRM_{-300\text{mT}}/SIRM$ . The  $S$ -ratio is a dimensionless parameter that indicates the content of ferrimagnetic (e.g., magnetite, titanomagnetite or maghemite) versus antiferromagnetic materials (e.g., hematite or goethite). Values close to +1 correspond to the predominance of ferrimagnetic material; on the other hand, values close to -1 correspond to antiferromagnetic materials. The  $ARM$  and  $IRM$  parameters were obtained using a spinner fluxgate magnetometer Minispin (Molspin Ltd.). Thermomagnetic analysis ( $\kappa-T$  heating curves using a system linked to MS3 meter, Bartington Ltd.) from room temperature to 650°C were performed over four selected samples with the aim of identify magnetic minerals.

Combining magnetic parameters graphically is very useful for assessing magnetic mineralogy. For example, the  $SIRM/\chi$  versus  $H_{cr}$  plot can be used to identify magnetic mineralogy (Peters and Dekkers, 2003). The  $\kappa_{ARM}$  versus  $\kappa$  plot (King et al., 1982) was used to identify the dominant size of the magnetic minerals. On the other hand, the  $\kappa_{ARM}/\kappa$  ratio (Dunlop and Özdemir, 1997) was also used to identify the presence of fine magnetite (< 0.1  $\mu$ m).

### 3.3. Chemical analysis

Trace elements (V, Ni, Cr and Zn) were determined using the LIBS technique (Laser Induced Breakdown Spectroscopy, Diaz Pace, 2002). A laser pulse (Nd:YAG, 100 mJ, temporal delay at 6  $\mu$ s, temporal width of 2  $\mu$ s) is focused onto the sample surface to produce a plasma (dielectric breakdown) that is analysed by spectroscopy. This technique is able to both identify and quantify trace elements (a few ppm), and it is a highly sensitive and low-cost method. For quantitative relation and calibration, seven soil samples were also measured using ICP-OES (*Martin et al., 1994*), and then for each element, calibration curves were made (i.e. concentration by ICP-OES against the LIBS signal).

### 3.4. Spatial and statistical analysis

The spatial continuity of magnetic, chemical variables, model dispersion output and the associated statistical parameters (PC) was investigated using the Moran's index ( $I$ ) (*Cressie, 1993*) and correlograms analysis. The  $I$  is a measure of spatial autocorrelation, i.e. how the values of a variable are related in the space based on the locations where they were measured. In the absence of spatial autocorrelation,  $I$  has an expected value of no autocorrelation given by  $E(I) = -1/(n-1)$ . The  $I$  values vary between -1 and +1, and  $I > E(I)$  indicate a positive autocorrelation, but  $I < E(I)$  indicates a negative autocorrelation. To determine whether a deviation of  $I$  from its expectation is statistically significant, one relies on the asymptotic distribution of  $I$ , which is a Gaussian distribution with a mean of  $-1/(n-1)$  and a variance of  $\sigma_I^2$ . The statistical hypothesis of no spatial autocorrelation is rejected at the  $\alpha$  significance level (in %) if  $|Z_{obs}| = |I - E(I)|/\sigma_I$  is more extreme than the  $Z_{\alpha/2}$  cut-off of a normal distribution,  $Z$  is a random variable of standard normal distribution. Correlograms were built by calculating the  $I$  for each variable at several lag distances.

The relationship between magnetic, chemical and model dispersion output variables was also studied using multivariate statistical analyses. Principal component analysis (PCA) was used as a tool for a variable reduction procedure in order to classify variables into groups with similar features. Canonical correlation analysis (CCA) was used for lineal association studies between variable sets.

Statistical analyses (Resume data, PCA and CCA) were made using the INFOSTAT® software (*Di Renzo et al., 2012*). The Moran's indexes were achieved with R language by the APE package.

## 4. RESULTS

### 4.1. The Gaussian Dispersion Model

Six geographic directions were used, and the Gaussian Dispersion Model (GDM) was obtained taking into account the temperature and velocity wind data. According to the Pasquill-Gifford classification, two atmospheric stability classes were identified for the study area, that is, type C and D. Then, for each sampling site, two dispersion model

**Table 1.** Statistics of trace elements of 27 samples.

	V [mg/kg]	Ni [mg/kg]	Cr [mg/kg]	Zn [mg/kg]
Mean	61.9	7.9	12.7	53.6
St.Dev.	7.0	4.3	1.0	20.6
Min	48.2	0.0	8.2	29.1
Max	76.1	17.3	14.3	95.2

results corresponding to C and D stability classes were evaluated. These results were studied jointly with other measured variables.

#### 4.2. Chemical analyses

There is scarce information about the heavy metals background for soils in the study area. *Lavado et al (2004)* reported Cr, Ni and Zn concentration (among others) of 13.21, 7.29 and 48.00 mg/kg, respectively, for soil type Luvic Phaeozem in this region (also classified as Argiudolls; *Pazos, 1996*). *Chaparro et al (2002)* reported Ni and Zn concentration of 10.5 and 26 mg/kg, respectively, for unpolluted soils from Tandil. Table 1 shows a summary of mean concentration for each measured element. The mean concentrations of Ni and Cr are very close to the reference values. Zn mean values are close to the Argiudolls soil types; however, the concentration was doubled with relation to the reported unpolluted soils from Tandil. There are no local vanadium reference values for comparison. The dust sample, collected close to the coke factory, does not show a higher V, Cr and Zn concentration than the soil samples; only the Ni concentration (17.3 mg/Kg) shows a substantial difference than the mean values in the soil samples. This finding may suggest that the largest proportion of this trace element would be released into the atmosphere in the form of gases, vapours and PM.

#### 4.3. Magnetic results

##### Magnetic mineral concentration

The mean and standard deviation (*St.Dev.*) values of  $\kappa_{is}$ ,  $\chi$ , *ARM* and *SIRM* are shown in Table 2. In-situ magnetic susceptibility values in unpolluted zones of Tandil are between  $39.0 \times 10^{-5}$  and  $167.0 \times 10^{-5}$  SI, according to *Chaparro et al (2002)*; in this study, the mean ( $\pm St.Dev.$ ) value of  $\kappa_{is}$  is  $(199.8 \pm 54.1) \times 10^{-5}$  SI and the maximum value is  $296.0 \times 10^{-5}$  SI. The mean  $\chi$  and *SIRM* values ( $182.3 \times 10^{-8} m^3/kg$  and  $19.4 mAm^2/kg$ , Table 2) are higher than those reported by *Chaparro et al (2002)*, i.e. between  $32$  and  $117 \times 10^{-8} m^3/kg$  for  $\chi$ , and between  $4.2$  and  $7.0 mAm^2/kg$  for *SIRM*. Magnetic enhancement seems to be evident at these sites; for example, the  $\kappa_{is}$  at several sites exceeds the above mentioned value for unpolluted zone by up to  $250 \times 10^{-5}$  SI and  $\chi$  by up to  $240 \times 10^{-8} m^3/kg$ . The sample collected around the coke factory shows the  $\chi$  value of  $76 \times 10^{-8} m^3/kg$  and the *SIRM* value of  $9.5 mAm^2/kg$ . It shows a strong magnetic signal; therefore, this material seems to be produced after the thermal heating process, which is because the raw material should be non-magnetic according to *Bidegain et al (2011)*.

**Table 2.** Statistics of magnetic parameters of 27 analysed samples.  $\kappa_{\text{is}}$ : in-situ magnetic susceptibility;  $\chi$ : mass-specific magnetic susceptibility;  $ARM$ : anhysteretic remanent magnetization;  $SIRM$ : saturation remanent magnetization;  $\kappa_{\text{fd}\%}$ : frequency-dependent magnetic susceptibility;  $\kappa_{\text{ARM}}$ : anhysteretic magnetic susceptibility;  $H_{cr}$ : coercivity of remanence.

	$\kappa_{\text{is}}$ [ $10^{-5}$ SI]	$\chi$ [ $10^{-8}$ m <sup>3</sup> /kg]	$ARM$ [ $10^{-6}$ Am <sup>2</sup> /kg]	$SIRM$ [mAm <sup>2</sup> /kg]	$\kappa_{\text{fd}\%}$ [%]	$\kappa_{\text{ARM}}/\kappa$	S-ratio	$H_{cr}$ [mT]
Mean	199.8	182.3	686.2	19.4	4.44	5.66	---	35.3
St.Dev.	54.1	46.1	216.1	4.1	2.36	1.02	---	1.6
Min	107.7	72.3	320.1	8.9	0.00	3.61	0.92	31.4
Max	296.2	272.7	1332.7	28.6	8.26	7.53	0.99	38.7

### Magnetic mineral and grain size identification

Magnetic characterization, i.e. magnetic mineralogy and grain size, was analysed from the  $IRM$  curves,  $\kappa_{\text{fd}\%}$ , S-ratio,  $H_{cr}$ ,  $SIRM/\chi$  and  $\kappa_{\text{ARM}}/\kappa$ . Both  $H_{cr}$  (mean 35.3 mT) and S-ratio values are shown in Table 2, which shows the predominance of ferrimagnetic materials, e.g. magnetite or maghemite. Thermomagnetic heating curves (Fig. 2c) also show a Curie temperature corresponding to magnetite with different contents of titanium. The biplot between the ratio  $SIRM/\chi$  and  $H_{cr}$  (Fig. 2b) also shows the predominance of magnetite-like grains in all samples.

According to Dearing *et al.* (1999), the  $\kappa_{\text{fd}\%}$  values between 2 and 10%, as found here, indicate a mixture of SP (grains size < 0.03 µm) and coarser non-SP grains. On the other hand, the  $\kappa_{\text{ARM}}/\kappa$ -ratio values indicate the presence of fine and ultra-fine magnetite. According to Peters and Dekkers (2003), the  $\kappa_{\text{ARM}}/\kappa$  versus magnetite grain size shows a peak-like behaviour, the highest values ( $\kappa_{\text{ARM}}/\kappa > 5$ ) occurring for very small

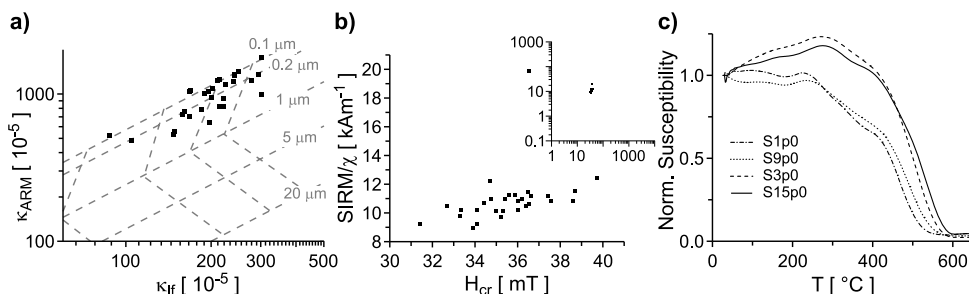


**Fig. 2.** a) King's Plot (King *et al.*, 1982); b)  $SIRM/\chi$  versus  $H_{cr}$  for all samples; c) Thermomagnetic heating curves of four selected samples.  $\kappa_{\text{if}}$ : volume-specific magnetic susceptibility;  $\kappa_{\text{ARM}}$ : anhysteretic magnetic susceptibility;  $SIRM$ : saturation remanent magnetization;  $\chi$ : mass-specific susceptibility;  $H_{cr}$ : coercivity of remanence;  $T$ : temperature.

magnetite grains (between 0.01 and 0.1  $\mu\text{m}$ ). In agreement with the previous analysis, the King's plot (Fig. 2a) evidences the predominance of magnetic minerals with magnetic grain sizes finer than 1  $\mu\text{m}$ . Therefore, the integrated analysis revealed the predominance of fine and ultra-fine ferrimagnetic minerals in all samples.

These studies about magnetic mineralogy and grain-size reveal similar values varying in a narrow range (e.g., the  $\text{mean} \pm \text{St.Dev.}$  of  $\kappa_{\text{ARM}}/\kappa$  and  $H_{cr}$  is  $5.66 \pm 1.02$  and  $35.3 \pm 1.6$  mT, respectively), and therefore a homogeneous magnetomineralogy is expected for most of the samples. On the other hand, as discussed previously, only magnetic concentration-dependent parameters have important variations in the study area.

#### 4.4. Statistical analysis

The multivariate statistical analysis was made in order to investigate the correlation between variables. The PCA was performed using standardized data of all measured variables ( $V$ ,  $\text{Ni}$ ,  $\text{Cr}$ ,  $\text{Zn}$ ,  $\kappa_{is}$ ,  $\chi$ ,  $ARM$ ,  $SIRM$ ,  $\kappa_{fd\%}$ ,  $\kappa_{\text{ARM}}/\kappa$ ,  $SIRM/\chi$ ,  $H_{cr}$  and S-ratio) and the output from model (Mod\_C and Mod\_D, corresponding to stability class C and D, respectively), and hence the correlation matrix.

From PCA results of the initial eigenvalues, three principal components (PC1 to PC3) were used, which accounted for over 68% of the total variance. The first component PC1 gathers mainly variables regarding to the magnetic concentration ( $\kappa_{is}$ ,  $\chi$ ,  $ARM$  and  $SIRM$ ) and the other two variables:  $H_{cr}$  and  $SIRM/\chi$ . Also, the  $V$  and  $\text{Cr}$  concentration in soils show a slightly positive correlation with PC1. The GDM output (Mod\_C and Mod\_D) shows a positive correlation with PC1 as well. The second one (PC2), comprised mainly the concentration of heavy metals ( $V$ ,  $\text{Ni}$ ,  $\text{Cr}$  and  $\text{Zn}$ ), and on the other hand, the third component (PC3) tends to group variables with regard to the magnetic grain sizes ( $\kappa_{\text{ARM}}/\kappa$  and  $\kappa_{fd\%}$  in lesser extent). The Mod\_D from GDM has a strong negative correlation with PC3. Results obtained from PCA are listed in Table 3. Fig. 3 shows the factor maps of variables where the same correlation behaviour between variables can be observed that was already shown in Table 3.

As regards CCA, four set of variables was considered and identified as ChG, CMG, MMG and GDM. In all cases, only the first pairs of canonical variables were taken into account. Firstly, an analysis between the chemical group ( $V$ ,  $\text{Ni}$ ,  $\text{Cr}$  and  $\text{Zn}$ , named ChG) and magnetic group (all measured magnetic parameters, named MG) was carried out, obtaining a canonical correlation  $R = 0.99$  that was statistically significant ( $p < 0.001$ ). Then, a new analysis dividing the MG was also tried; for this purpose, the MG was divided into two groups regarding the relevance of variables contributing to the relationship. Thus, one group was made using the concentration-dependent magnetic parameters (CMG:  $\kappa_{is}$ ,  $\chi$ ,  $ARM$  and  $SIRM$ ) and the other one using the mineralogy-dependent magnetic parameters (MMG:  $\kappa_{\text{ARM}}$ , S-ratio,  $H_{cr}$ ,  $\kappa_{\text{ARM}}/\kappa$  and  $\kappa_{fd\%}$ ). This new analysis yielded different canonical correlations, that is, a statistically insignificant correlation ( $p = 0.06$ ) between ChG and CMG, and  $R = 0.96$  (statistically significant,  $p < 0.001$ ) between ChG and MMG. Such results show a significant canonical correlation for the group corresponding feature-dependent magnetic parameters and chemical variables. On the other hand, the fourth group involving dispersion model results (GDM:

**Table 3.** Correlation coefficients between first three components of the principal component analyses (PC1, PC2 and PC3) and measured variables.  $\kappa_{\text{is}}$ : in-situ magnetic susceptibility;  $\chi$ : mass-specific magnetic susceptibility;  $ARM$ : anhysteretic remanent magnetization;  $SIRM$ : saturation remanent magnetization;  $\kappa_{\text{fd}\%}$ : frequency-dependent magnetic susceptibility;  $\kappa_{\text{ARM}}$ : anhysteretic magnetic susceptibility;  $H_{cr}$ : coercivity of remanence; MOD\_C and MOD\_D: output from the Gaussian Dispersion Model. The asterisk denotes the best correlation obtained for the corresponding principal component.

	PC1	PC2	PC3
V	0.62*	0.53*	-0.34
Ni	0.33	0.75*	0.24
Cr	0.71*	0.55*	0.20
Zn	0.28	0.69*	-0.06
$\kappa_{\text{is}}$	0.80*	-0.41	0.04
$\chi$	0.92*	-0.22	0.08
$ARM$	0.83*	-0.39	0.21
$SIRM$	0.84*	-0.40	-0.08
$\kappa_{\text{fd}\%}$	-0.04	-0.26	0.42
$\kappa_{\text{ARM}}/\kappa$	0.46	0.06	0.69*
$SIRM/\chi$	-0.67*	-0.31	0.12
$H_{cr}$	-0.63*	0.44	0.12
S-ratio	0.26	-0.23	-0.24
Mod_C	0.68*	0.03	-0.47
Mod_D	0.50*	0.19	-0.65*

Mod\_C and Mod\_D) shows a significant canonical correlation with both the CMG ( $R = 0.70, p < 0.05$ ) group and the ChG ( $R = 0.79, p < 0.01$ ).

Moran's index results for PC1, PC2, PC3 and all measured spatial variables using different distance lags were achieved. The heavy metals, in particular vanadium and zinc, showed significant autocorrelation according to their  $p$  value ( $< 0.05$ ). Magnetic concentration dependent variables showed a very good autocorrelation index for  $\chi$  and SIRM was statistically significant ( $p < 0.05$ ). Furthermore, the PC1 shows a statistically significant  $I$  ( $p < 0.01$ ); this result is indicative that the PC1, and its involved variables group, has an excellent spatial dependence.

Correlograms for some variables are shown in Fig. 4. In general, similar results are observed for different distance lags in comparison to the previous analysis. The PC1 correlogram is similar to the correlograms corresponding to the magnetic concentration variables and the GDM output for the D stability class (Mod\_D). A different pattern (a peak-like curve) is observed for the PC2 correlogram, which is similar to the correlograms of trace elements and the GDM output for the C stability class (Mod\_C). In the last case, the spatial continuity rises reaching the maximum values at 500–1000 m. The correlograms for other magnetic variables are not shown here because they were not significant, except for  $H_{cr}$ . Only the remanence coercivity has a very good spatial continuity, which is interpreted as the spatial homogeneity of the magnetic minerals.

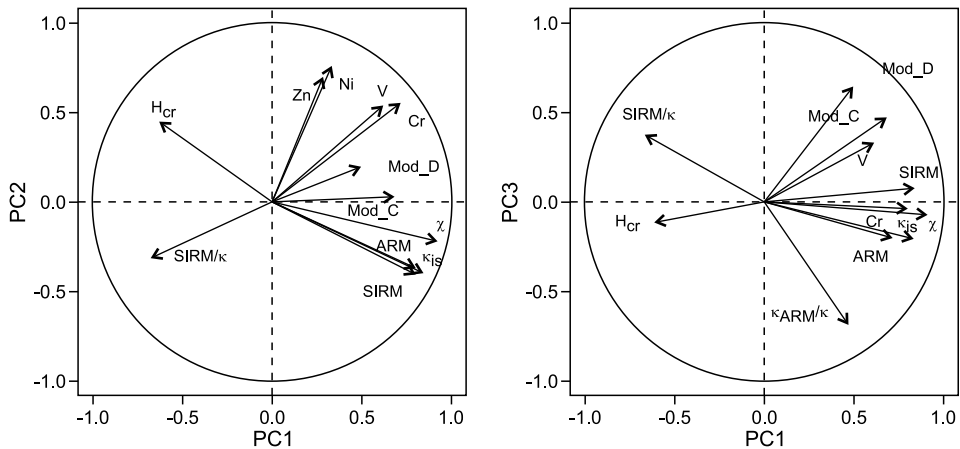


**Fig. 3.** Variable factor maps from the principal component analysis for the first three principal components PC1, PC2 and PC3, describing 38.63%, 17.43% and 11.92% of the data variability, respectively.  $\kappa_{is}$ : in-situ magnetic susceptibility;  $\chi$ : mass-specific magnetic susceptibility; *ARM*: anhysteretic remanent magnetization; *SIRM*: saturation remanent magnetization;  $\kappa_{fd\%}$ : frequency-dependent magnetic susceptibility;  $\kappa_{ARM}$ : anhysteretic magnetic susceptibility;  $H_{cr}$ : coercivity of remanence.

## 5. DISCUSSION

In this small study area, it is assumed that there is a unique geomorphological unit and lithological contribution to the soil's magnetic properties. In addition, the magnetic mineralogy of the PM emission should be homogeneous or, at least, with slight variation. The magneto-mineralogical analysis shows that magnetite is the main magnetic carrier and no other additional magnetic phase seems to be present. Although the magnetic grain sizes (e.g.,  $\kappa_{ARM}/\kappa$  and  $\kappa_{fd\%}$ ) and magnetic mineralogy (e.g.,  $H_{cr}$  and  $SIRM/\chi$ ) remain relatively constant in the study area, the magnetic concentration varies with distance and from the pollution source. Therefore, the PM emission from the coke factory seems to show evidence of ferrimagnetic minerals accumulated in nearby soils; in this case, the pollution influence of the cooking production only gives an enhancement of concentration-dependent magnetic parameters and the PM content. The distribution maps represented in Fig. 5 shows the following: a) the GDM output for C atmospheric stability class and b) the PC1 variable mainly made by magnetic concentration-dependent variables. In both figures, it can be observed how the central region from Southwest to Northeast evidences the highest impact of pollutants.

The PCA reveals, in a multivariate way, three variables groupings from the one-to-one relationships between variables. Magnetic variables are grouped in two components (PC1 and PC3) as well as the GDM variables (Mod\_C mainly and to a lesser extent Mod\_D). In this way, it is worth notice how concentration-dependent magnetic parameters ( $\kappa_{is}$ ,  $\chi$ ,

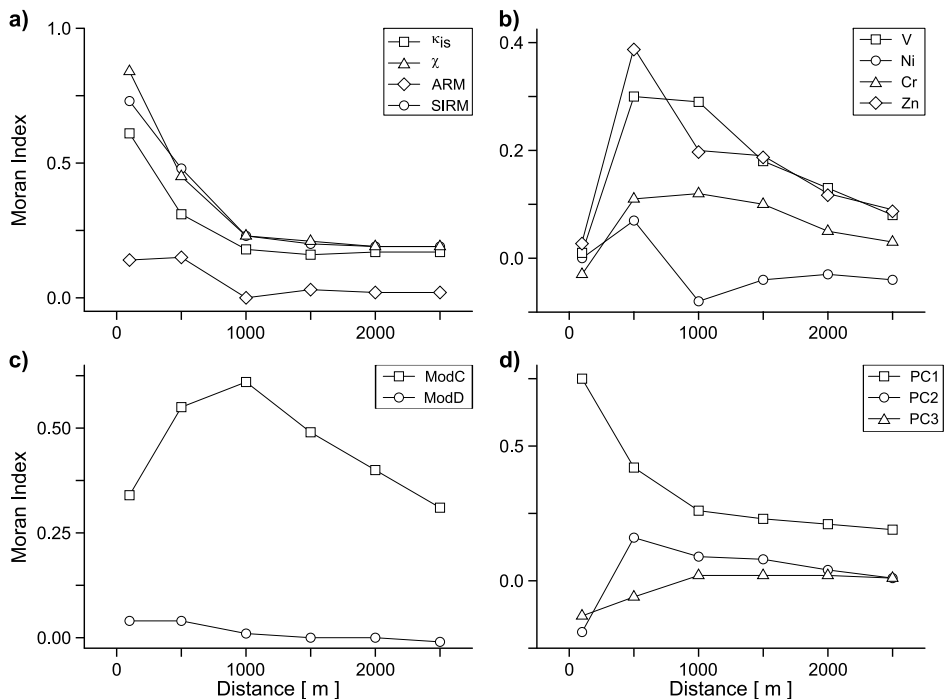


**Fig. 4.** Correlograms for **a)** magnetic variables, **b)** trace elements, **c)** modelled Gaussian Dispersion Model (Mod\_C and Mod\_D) of particulate matter emissions, and **d)** principal components (PC1–3).  $\kappa_{is}$ : in-situ magnetic susceptibility;  $\chi$ : mass-specific magnetic susceptibility; ARM: anhysteretic remanent magnetization; SIRM: saturation remanent magnetization.

*ARM* and *SIRM*), V, Cr and GDM show positive correlation and contribute to the construction of the first PC (PC1). From a mineralogical point of view, taking into account previous analyses, an increase of (titano-)magnetite concentration is related to areas with higher PM concentration predicted by the GDM. In spite of V and Cr showing positive correlations with PC1, the four analysed trace elements contribute to the construction of the second PC (PC2). This could suggest an input of another pollution source (vehicular emission).

The CCA shows that the plume dispersion model GDM, has a statistically significant canonical correlation ( $R = 0.70$ ;  $p < 0.05$ ) with concentration-related magnetic parameters (CMG). Although the statistical procedures explain a similar variance percentage, the CCA is a way of quantifying the linear relationship between two groups of multidimensional variables (Chaparro *et al.*, 2008).

According to the CCA coefficients for both correlated groups - CMG and GDM - the *SIRM* has a strong influence over the CMG. The  $\kappa_{is}$  has a negative coefficient, although smaller than *SIRM*. On the other hand, both Mod\_C and Mod\_D have a similar influence over GDM, but they have negative and positive coefficients, respectively. In this way,

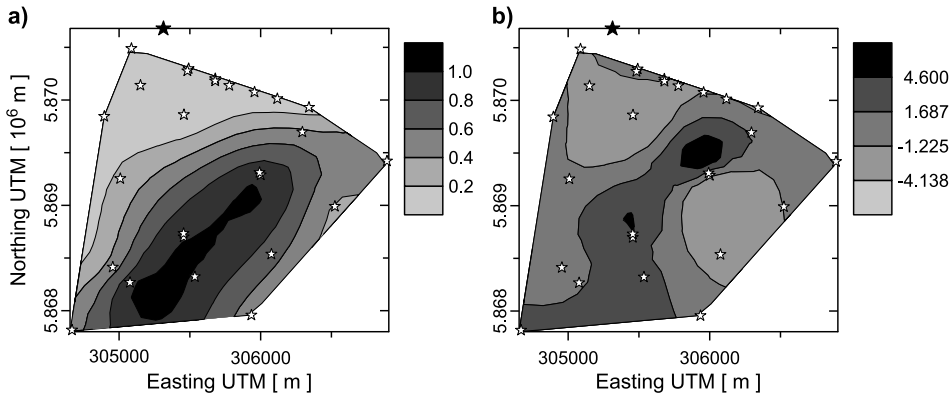


**Fig. 5.** Distribution pollution maps (dimensionless) from **a)** Gaussian Dispersion Model (stability class C, normalized with respect to the maximum concentration obtained) and **b)** scores of the first principal component constructed mainly for concentration-dependent magnetic parameters. The coke factory position is represented by a black star.

areas closer to the factory where unstable atmospheric conditions (stability class C) prevail over other conditions and they are also more affected by coarse PM deposition, there tends to be a positive correlation between Mod\_C and  $\kappa_{is}$ . On the contrary, sites away from the factory, where more stable atmospheric conditions (stability class D) prevail, the Mod\_D is more positively correlated with SIRM.

Correlograms built from Moran's indexes for several distance lags have shown positive spatial clusters association for most of the measured variables and for the C stability class from the GDM. The correlograms of concentration-dependent magnetic parameters ( $\kappa_{is}$ ,  $\chi$  and SIRM) show similar behaviour to the PC1. In such a case, the spatial continuity is statistically significant for all distance lags; however, the PC1 falls importantly from maximum values between small distance lags and 1000 m, and between 1000 and 2500 m a slight decrease is observed. On the other hand the trace elements V, Zn and Cr show similar behaviour to PC2 with maximum spatial continuity around a distance of 500–1000 m, but without spatial continuity for close distances. This spatial discontinuity of the small scale is a result of the high variability of trace elements (in terms of standard deviation), which may be due to other pollution sources (for example: vehicular emission) without important influence and not considered in this study. Finally, most of these variables fall slightly and V, Cr and Zn have non-spatial continuity beyond 1500–2500 m.

## 6. CONCLUSIONS

In this work, the PM atmospheric distribution was studied in soil samples through a set of magnetic and chemical techniques and using a simple dispersion model. The study focused on magnetic properties of soil that have shown advantages in this kind of pollution study. The results show the possibility of monitoring the environmental PM distribution using magnetic techniques applied in soils or different PM collector types.

According to the PCA, the GDM used here has shown a good association with magnetic parameters. In this sense, it is worth noticing the positive correlation between concentration-dependent magnetic parameters and both GDM considered. On the other hand, and according to the CCA results, the deposition of fine PM tends to be better represented by the SIRM and the coarse PM by the magnetic susceptibility. However, the latter fact depends on the particular characteristics of the pollution source and the model construction leading to a more refined GDM that takes into account the contribution of coarse PM.

*Acknowledgements:* The authors wish to thank the UNCPBA and CONICET for their financial support and the LIBS Laboratory (CIFICEN-UNCPBA) for the measurement of heavy metals. And finally, we give special thanks to Dr. Mauro A. E. Chaparro for his help in the statistical analysis. We also thank both anonymous reviewers for their constructive comments that helped to improve this manuscript.

#### *References*

- Bidegain J.C., Chaparro M.A.E., Marié D.C. and Jurado S., 2011. Air pollution caused by manufacturing coal from petroleum coke in Argentina. *Environ. Earth Sci.*, **62**, 847–855.
- Blundell A., Hannam J.A., Dearing J.A. and Boyle J.F., 2009. Detecting atmospheric pollution in surface soils using magnetic measurements: A reappraisal using an England and Wales database. *Environ. Pollut.*, **157**, 2878–2890.
- Chaparro M.A.E., 2006. *Estudio de Parámetros Magnéticos de Distintos Ambientes Relativamente Contaminados en Argentina y Antártida (Study of Magnetic Parameters of Several Relatively Polluted Sites from Argentina and Antarctica)*. Monografía No. 7, Geofísica UNAM, México (in Spanish).
- Chaparro M.A.E., Chaparro M.A.E., Marinelli C. and Sinito A.M., 2008. Multivariate techniques as alternative statistical tools applied to magnetic proxies for pollution: A case study from Argentina and Antarctica. *Environ. Geol.*, **54**, 365–371.
- Chaparro M.A.E., Chaparro M.A.E. and Sinito A.M., 2012. An interval fuzzy model for magnetic monitoring: Estimation of a pollution index. *Environ. Earth Sci.*, **66**, 1477–1485.
- Chaparro M.A.E., Gogorza C.S.G., Chaparro M.A.E., Irurzun M.A. and Sinito A.M., 2006. Review of magnetism and heavy metal pollution studies of various environments in Argentina. *Earth Planets Space*, **58**, 1411–1422.
- Chaparro M.A.E., Nuñez H., Lirio J.M., Gogorza C.S.G. and Sinito A.M., 2007. Magnetic screening and heavy metal pollution studies in soils from Marambio Station, Antarctica. *Antarctic. Sci.*, **19**, 379–393.
- Charlesworth S.M. and Lees J.A., 2001. The application of some mineral magnetic measurements and heavy metal analysis for characterising fine sediments in an urban catchment, Coventry, UK. *J. Appl. Geophys.*, **48**, 113–125.
- Conner T.L., Norris G.A., Landis M.S. and Williams R.W., 2001. Individual particle analysis of indoor, outdoor, and community samples from the 1998 Baltimore particulate matter study. *Atmos. Environ.*, **35**, 3935–3946.
- Cressie N.A., 1993. *Statistics for Spatial Data*. Revised Edition. John Wiley and Sons, New York.

- Dearing J., 1999 Magnetic susceptibility. In: Walden J., Oldfield F. and Smith J. (Eds), *Environmental Magnetism: a Practical Guide*. Technical Guide No 6. Quaternary Research Association, London, U.K., 35–62.
- Di Rienzo J.A., Casanoves F., Balzarini M.G., Gonzalez L., Tablada M. and Robledo C.W., 2012. INFOSTAT® (Version 2012). Grupo InfoStat, FCA, Universidad Nacional de Córdoba, Córdoba, Argentina ([www.infostat.com.ar](http://www.infostat.com.ar)).
- Diaz Pace D., 2002. *Técnica LIBS para la Detección de Trazas en Suelos Mediante Análisis Espectroscópico considerando Líneas Absorbidas por el Plasma (LIBS Technique for Trace Element Detection in Soils Using Spectroscopy Analysis Considering Absorbed Lines for Plasmas)*. PhD Thesis. Fac. Exactas, UNCPBA, Tandil, Argentina (in Spanish).
- Dunlop D.J. and Özdemir Ö., 1997. *Rock Magnetism. Fundamentals and Frontiers*. Cambridge Univ. Press, Cambridge, U.K.
- Ďurža O., 1999. Heavy contamination and magnetic susceptibility in soils around metallurgical plant. *Phys. Chem. Earth A*, **24**, 541–543.
- Flanders P.J., 1994. Collection, measurement, and analysis of airborne magnetic particulates from pollution in the environment. *J. Appl. Phys.*, **75**, 5931–5936.
- Gifford F.A., 1961. Uses of routine meteorological observation for estimating atmospheric dispersion. *Nuclear Safety*, **2(4)**, 47–51.
- Hanesch M. and Scholger R., 2002. Mapping of heavy metal loadings in soils by means of magnetic susceptibility measurements. *Environ. Geol.*, **42**, 857–870.
- Heller F., Strzyszcz Z. and Magiera T., 1998. Magnetic record of industrial pollution in soils of Upper Silesia, Poland. *J. Geophys. Res.*, **103(B8)**, 17767–17774.
- Henke K., 2005. Trace element chemistry of fly ashes from co-combusted petroleum coke and coal. Paper #45. International Ash Utilization Symposium, Center for Applied Energy Research, University of Kentucky, Lexington, KY (<http://www.flyash.info/2005/11hen.pdf>).
- Hower J.C., Thomas G.A., Mardon S.M. and Trimble A.S., 2005. Impact of co-combustion of petroleum coke and coal on fly ash quality: Case of study of a Western Kentucky power plant. *Appl. Geochem.*, **20**, 1309–1319.
- Hunt A., Jones J. and Oldfield F., 1984. Magnetic measurements and heavy metals in atmospheric particulates of anthropogenic origin. *Sci. Tot. Environ.*, **33**, 129–139.
- Jordanova N.V., Jordanova D.V., Veneva L., Yorova K. and Petrovský E., 2003. Magnetic response of soils and vegetation to heavy metal pollution - a case study. *Environ. Sci. Technol.*, **37**, 4417–4424.
- Kapička A., Petrovský E., Ustjak S. and Macháčková K., 1999. Proxy mapping of fly-ash pollution of soils around a coal-burning power plant: A case study in Czech Republic. *J. Geochem. Explor.*, **66**, 291–297.
- King J., Banerjee S.K., Marvin J. and Özdemir Ö., 1982. A comparison of different magnetic methods for determining the relative grain size of magnetite in natural materials: Some results from lake sediments. *Earth Planet. Sci. Lett.*, **59**, 404–419.
- Lavado R.S., Zubillaga M.S., Alvarez R. and Taboada M., 2004. Baseline levels of potentially toxic elements in Pampa soils. *Soil Sediment. Contam.*, **13**, 427–437.

- Liu G., Liu W., Cai Z. and Zheng M., 2013. Concentrations, profiles, and emission factors of unintentionally produced persistent organic pollutants in fly ash from coking processes. *J. Hazard. Mater.*, **261**, 421–426.
- Lu S.G. and Bai S.Q., 2006. Study on the correlation of magnetic properties and heavy metals content in urban soils of Hangzhou City, China. *J. Appl. Geophys.*, **60**, 1–12.
- Magiera T., Strzyszcz Z., Kapička A., Petrovský E. and MAGPROX Team, 2006. Discrimination of lithogenic and anthropogenic influences on topsoil magnetic susceptibility in Central Europe. *Geoderma*, **130**, 299–311.
- Maher B., Moore C. and Matzka J., 2008. Spatial variation in vehicle-derived metal pollution identified by magnetic and elemental analysis of roadside tree leaves. *Atmos. Environ.*, **42**, 364–373.
- Martin, D.O., 1976. Comment on change of concentration standard deviations with distance. *J. Air Pollut. Contr. Assoc.*, **26**, 145–146.
- Nelson H.W., 1970. *Petroleum Coke Handling Problem*. [https://web.anl.gov/PCS/acsfuel/preprint%20archive/Files/13\\_4\\_NEW%20YORK\\_09-69\\_0121.pdf](https://web.anl.gov/PCS/acsfuel/preprint%20archive/Files/13_4_NEW%20YORK_09-69_0121.pdf).
- Pasquill F., 1961. The estimation of the dispersion of windborne material. *Meteorol. Mag.*, **90**, 33–49.
- Pazos M.S., 1996. Classification of soils of Azul county (Buenos Aires Province, Argentina) according to the World Reference Base for Soil Resources (ISSS, ISRIC, FAO, 1994). *Cienc. del Suelo*, **14**, 116–118.
- Pazos M.S. and Mastelan S.A., 2001. Influence of the change from herbaceous to arboreal vegetation on some properties of luvic phaeozem soils exposed to cattle management. *Información Tecnológica*, **12(2)**, 19–25.
- Peters C. and Dekkers M.J., 2003. Selected room temperature magnetic parameters as a function of mineralogy, concentration and grain size. *Phys. Chem. Earth*, **28**, 659–667.
- Rachwał M., Magiera T. and Wawer M., 2015. Coke industry and steel metallurgy as the source of soil contamination by technogenic magnetic particles, heavy metals and polycyclic aromatic hydrocarbons. *Chemosphere*, **138**, 863–873.
- Schibler L., Boyko T., Ferdyn M., Gajda B., Höll S., Jordanova N., Rösler W. and MAGPROX Team, 2002. Topsoil magnetic susceptibility mapping: Data reproducibility and compatibility, measurement strategy. *Stud. Geophys. Geod.*, **46**, 43–57.
- Strzyszcz Z., 1993. Magnetic susceptibility of soils in the areas influenced by industrial emission. In: Schulin R., Webster R., Desaules A. and Steiger W. (Eds), *Soil Monitoring*. Monte Verita: Proceedings of the Centro Stefano Franscini. Birkhäuser Verlag, Basel, Switzerland, 255–269.
- Strzyszcz Z., Magiera T. and Heller F., 1996. The influence of industrial immissions on the magnetic susceptibility of soils in Upper Silesia. *Stud. Geophys. Geod.*, **40**, 276–286.
- Thompson R. and Oldfield F., 1986. *Environmental Magnetism*. Allen and Unwin, London, U.K.
- Martin T.D., Brockhoff C.A., Creed J.T. and EMMC Methods Work Group, 1994. Determination of trace elements in waters and wastes by inductively coupled plasma-atomic emission spectrometry. Method 200.7, Revision 4.4. In: *Method for the determination of metals in environmental samples - Suplement 1*. US-EPA/600/R-94/111. United States Environmental Protection Agency, Cincinnati, OH.